

Prognostic Stratification of Metastatic Gastroenteropancreatic Neuroendocrine Neoplasms by ^{18}F -FDG PET: Feasibility of a Metabolic Grading System

Samer Ezziddin¹, Linda Adler¹, Amir Sabet¹, Thorsten Dirk Pöppel², Florian Grabellus³, Ali Yüce⁴, Hans-Peter Fischer⁵, Birgit Simon⁶, Tobias Höller⁷, Hans-Jürgen Biersack¹, and James Nagarajah²

¹Department of Nuclear Medicine, University Hospital Bonn, Bonn, Germany; ²Department of Nuclear Medicine, University Hospital Essen, Essen, Germany; ³Institute of Pathology, University Hospital Essen, Essen, Germany; ⁴Department of Internal Medicine, University Hospital Essen, Essen, Germany; ⁵Institute of Pathology, University Hospital Bonn, Bonn, Germany; ⁶Department of Radiology, University Hospital Bonn, Bonn, Germany; and ⁷Institute of Medical Biometry, Informatics, and Epidemiology, Bonn, Germany

The tumor proliferation marker, Ki-67 index, is a well-established prognostic marker in gastroenteropancreatic neuroendocrine neoplasms (NENs). Noninvasive molecular imaging allows whole-body metabolic characterization of metastatic disease. We investigated the prognostic impact of ^{18}F -FDG PET in inoperable multifocal disease. **Methods:** Retrospective, dual-center analysis was performed on 89 patients with histologically confirmed, inoperable metastatic gastroenteropancreatic NENs undergoing ^{18}F -FDG PET/CT within the staging routine. Metabolic (PET-based) grading was in accordance with the most prominent ^{18}F -FDG uptake (reference tumor lesion): mG1, tumor-to-liver ratio of maximum standardized uptake value ≤ 1.0 ; mG2, 1.0–2.3; mG3, >2.3 . Other potential variables influencing overall survival, including age, tumor origin, performance status, tumor burden, plasma chromogranin A (≥ 600 $\mu\text{g/L}$), neuron-specific enolase (≥ 25 $\mu\text{g/L}$), and classic grading (Ki-67–based) underwent univariate (log-rank test) and multivariate analysis (Cox proportional hazards model), with a *P* value of less than 0.05 considered significant. **Results:** The median follow-up period was 38 mo (95% confidence interval [CI], 27–49 mo); median overall survival of the 89 patients left for multivariate analysis was 29 mo (95% CI, 21–37 mo). According to metabolic grading, 9 patients (10.2%) had mG1 tumors, 22 (25.0%) mG2, and 57 (64.8%) mG3. On multivariate analysis, markedly elevated plasma neuron-specific enolase (*P* = 0.016; hazard ratio, 2.9; 95% CI, 1.2–7.0) and high metabolic grade (*P* = 0.015; hazard ratio, 4.7; 95% CI, 1.2–7.0) were independent predictors of survival. **Conclusion:** This study demonstrated the feasibility of prognostic 3-grade stratification of metastatic gastroenteropancreatic NENs by whole-body molecular imaging using ^{18}F -FDG PET.

Key Words: PET/CT; ^{18}F -FDG; gastroenteropancreatic; neuroendocrine tumors; prognostic stratification; tumor grading

J Nucl Med 2014; 55:1260–1266

DOI: 10.2967/jnumed.114.137166

Received Jan. 6, 2014; revision accepted Apr. 1, 2014.
For correspondence or reprints contact: Samer Ezziddin, Department of Nuclear Medicine, University Hospital Bonn, Sigmund-Freud-Strasse 25, D-53105 Bonn, Germany.
E-mail: samer.ezziddin@ukb.uni-bonn.de
Published online May 29, 2014.
COPYRIGHT © 2014 by the Society of Nuclear Medicine and Molecular Imaging, Inc.

Prognostication of gastroenteropancreatic neuroendocrine tumors (NETs) is a relevant topic for patient management; tumor proliferation–derived grading is now implemented into the classification system of neuroendocrine neoplasms (NENs) according to the current European Neuroendocrine Tumor Society guidelines (1–3). This classification divides tumors into 3 grades, G1–G3, according to the proliferation index, also termed Ki-67 index, with G1 being defined as a Ki-67 index of less than 3%, G2 as 3%–20%, and G3 as greater than 20%. Although the differentiation of G1 from G2 helps to predict the tendency of the tumor to metastasize, the differentiation of G1–G2 from G3 profoundly guides treatment of metastatic patients—for example, implementation of first-line chemotherapy versus less aggressive treatment such as somatostatin analogs (4–6). Response to treatment may be homogeneous within the entire G1–G2 range (7), but outcome of uniformly treated metastatic NENs is still influenced by the proliferation index, even within the G1–G2 range (8,9).

The invasive nature of the biopsy procedure limits the proliferation evaluation (Ki-67 index determination) and makes assessments from multiple sites and recurrent time points difficult to implement in practice. A heterogeneous or changing proliferation status may thus yield different proliferation indices depending on the site or timing of the biopsy during the disease. In light of these potential inaccuracies, molecular imaging–derived grading tools could possibly supplement histopathologic grading in metastatic disease; moreover, the site of biopsy might be guided by such an imaging tool if proven to be of prognostic relevance. It is conceivable that tumor grading in multifocal metastatic disease may be significantly improved by such a whole-body imaging approach; it would facilitate individualized treatment and allow personalized medicine (10).

^{18}F -FDG is a radiochemically modified, positron-emitting glucose analog that allows metabolic PET imaging depicting the glycolytic activity of tumors, thus characterizing viability and malignant potential. ^{18}F -FDG PET imaging has been shown to prognosticate survival in various tumor entities (11,12). Especially in tumors with variable ^{18}F -FDG uptake, such as hepatocellular carcinoma (13,14), prostate cancer (15,16), and gastrointestinal stroma tumors (17,18), a correlation between ^{18}F -FDG avidity and biologic behavior of the tumor (indicated by patient survival) has been shown to facilitate outcome prediction or metabolic

grading by noninvasive measures. Recent studies have also shown such value for NENs (19,20).

With the growing diversity of treatment options and various aggressive approaches in NENs, especially in advanced metastatic disease, predictors of outcome become more important for patient management and selection of adequate therapeutic options. We aimed to assess the prognostic power of patient stratification in inoperable metastatic disease by ^{18}F -FDG PET and to compare it with other conventional prognostic variables, including the Ki-67 index; the outcome variable was overall survival in a consecutive patient population with inoperable metastatic disease for which ^{18}F -FDG PET/CT was implemented in the diagnostic work-up.

MATERIALS AND METHODS

We retrospectively analyzed a consecutive patient cohort with histologically confirmed gastroenteropancreatic TNM stage IV NENs and inoperable metastatic disease undergoing ^{18}F -FDG PET/CT as part of the staging routine. The institutional review boards of both University Bonn and University Duisburg-Essen approved this retrospective study, and the requirement to obtain informed consent was waived.

Patients

The patient cohort consisted of 89 consecutive patients (mean age, 65 y; range, 31–83 y; 47 men and 42 women) with TNM stage IV NENs of the gastrointestinal and pulmonary tracts, formerly named gastroenteropancreatic NET, according to the current World Health Organization classification. Inclusion criteria for retrospective evaluation were histologically confirmed gastroenteropancreatic NENs, verified metastatic disease (TNM stage IV) with inoperable spread and a completed ^{18}F -FDG PET/CT examination, and available histopathology and follow-up data. The patients' characteristics are listed in Table 1. Thirty-one patients had pancreatic NENs, and 57 patients had nonpancreatic gastrointestinal NENs, of which 15 were foregut (11 with pulmonary primary), 16 midgut, 4 hindgut, and 22 gastroenteropancreatic with an unknown primary. Metastatic sites included the liver in 74 patients (83%), bone in 38 (42%), and other organs in 49 (55%). Previous treatments comprised surgery ($n = 33$ [38%]), biotherapy ($n = 18$ [21%]), chemotherapy ($n = 21$ [24%]), locoregional treatment ($n = 2$ [2%]), and peptide receptor radionuclide therapy ($n = 32$ [37%]). Hepatic tumor load at the time of imaging was categorized according to the CT scan: no hepatic tumor, less than 25% liver involvement, 25%–50% involvement, and more than 50% involvement. There were no significant differences in these parameters between the 2 cohorts ($P > 0.2$).

Histopathology and Tumor Grading

Patients were classified according to the current TNM staging and grading system for NENs (1,2,21). All tumors were NENs with distant metastases (TNM stage IV). Histopathology and immunohistochemical analyses, including determination of the Ki-67 proliferation index, were performed on resection specimens or biopsy material. According to consensus recommendations, the Ki-67 index was expressed as the percentage of MIB1 antibody-stained tumor cells in the areas of highest nuclear labeling (1,2). The current definition of NEN grading was used, with a Ki-67 index of less than 3%, 3%–20%, and more than 20% for G1, G2, and G3, respectively. These categories were also termed pG1, pG2, and pG3 to differentiate them from the metabolic grading classes (mG1, mG2, mG3) derived from PET imaging. The interval between the latest Ki-67 index determination and PET imaging was 8.4 ± 6.5 mo.

^{18}F -FDG PET/CT and Tracer Uptake Quantification

In both participating institutions, PET/CT was performed with the same integrated scanner (Biograph 2; Siemens Medical Solutions) and

TABLE 1
Patients' Characteristics at Baseline PET/CT

Variable	n	%
Total number of patients	89	100
Sex		
Male	47	53
Female	42	47
Age (mean, 65 y; range, 31–83 y)		
≤ 65 y	51	57
> 65 y	38	43
Tumor origin	88	100
Pancreatic NENs	31	35
Gastrointestinal NENs	35	41
Foregut	15	17
Midgut	16	18
Hindgut	4	5
Unknown primary	22	25
Grade (Ki-67 index)	80	100
G1 ($\leq 2\%$)	16	20
G2 (3%–20%)	46	58
G3 ($> 20\%$)	18	22
Karnofsky performance status	68	100
> 70	48	71
≤ 70	20	29
Tumor burden (liver)	85	100
None	13	15
$< 25\%$	50	59
25%–50%	13	15
$> 50\%$	9	11
Bone involvement	87	100
Yes	38	44
No	49	56
Chromogranin A	59	100
< 600 $\mu\text{g/L}$	33	56
≥ 600 $\mu\text{g/L}$	26	44
NSE	59	100
< 25 $\mu\text{g/L}$	35	59
≥ 25 $\mu\text{g/L}$	24	41
Previous treatment	86	100
None	31	36
Any	55	64
Surgery	33	38
Chemotherapy	21	24
Biotherapy	18	21
Locoregional treatment	2	2
Peptide receptor radionuclide therapy	32	37

the same acquisition protocol. There were no significant differences in time to acquisition or amount of injected ^{18}F -FDG activity. The scanners were calibrated according to national quality control standards, and the same image reconstruction algorithms were used, providing comparable interinstitutional standardized uptake values (SUVs). The patients fasted for at least 6 h before ^{18}F -FDG administration, and blood glucose levels were less than 200 mg/dL at the time of injection. The scans were acquired from the base of the skull to the upper thighs (5–7 bed positions) 60–90 min after injection of 300–400 MBq of ^{18}F -FDG. Small bowel was delineated by administration of 1 L of diluted ionic oral contrast material 30–60 min before the examination. The hybrid PET/CT scanner consisted of a dual-detector helical CT scanner and a high-resolution PET scanner with a 16.2-cm axial field of view and lutetium oxyorthosilicate crystal detectors ($6.45 \times 6.45 \times 25$ mm). CT was performed for attenuation correction and anatomic localization using the following parameters: 60 mAs; 130 kV; 0.8 s/tube

rotation; slice thickness, 5 mm; slice width, 5 mm; and table feed, 8 mm/s. For vascular and parenchymal delineation, 140 mL of iodinated contrast material (Ultravist 300; Schering) was administered using an automated injector (XD 5500; Ulrich Medical Systems) with a start delay of 50 s. Immediately after the CT image acquisition, PET data were acquired for 5 min per bed position. The coincidence time resolution was 500 ps, with a coincidence window of 4.5 ns. The sensitivity was 5.7 cps/kBq at 400 keV. The attenuation-corrected PET data underwent standardized ordered-subset expectation maximization iterative reconstruction with 2 iterations and 8 subsets and a 5-mm gaussian filter.

The SUV was determined as a measure of ^{18}F -FDG uptake using a region-of-interest technique. Tumors with the highest SUV (SUV_{max}) were selected as target lesions, and the normal liver parenchyma was selected as background control. To normalize tumor SUV, the ratio of SUV_{max} of the tumor lesion to that of normal liver parenchyma, or tumor-to-liver (T/L) ratio, was calculated. To reduce potential partial-volume effects, the reference region of interest in the liver was kept consistently at 2 cm in diameter.

Outcome and Statistical Analysis

The baseline characteristics of the study population were analyzed with regard to survival outcome. The measure of outcome was overall survival from baseline evaluation, which included the ^{18}F -FDG PET/CT study. Each factor was dichotomized or scaled within a 3-grade stratification system; overall survival was analyzed using the Kaplan–Meier method (log-rank test with $P < 0.05$). Multivariate analysis (Cox proportional hazards) with the stepwise model by backward elimination was performed with those variables that had proven significant on univariate analysis (log-rank test). All tests were performed with a 2-sided P value of less than 0.05 considered significant. The statistical software package SPSS (version 18.0; SPSS Inc.) was used to analyze the data.

RESULTS

The median follow-up period was 38 mo (95% confidence interval [CI], 27–49 mo). The median overall survival of the entire cohort ($n = 89$) was 29 mo (95% CI, 21–37). Forty-six patients (51.7%) had died by the end of the study. Metabolic grading of tumor lesions via ^{18}F -FDG PET (T/L ratio of $\text{SUV}_{\text{max}} \leq 1.0$, 1.0–2.3, or >2.3) identified 9 patients (10.2%) with mG1 tumors, 22 (25.0%) with mG2, and 57 (64.8%) with mG3. Patient examples from different metabolic grading classes, with outcomes and respective imaging results, are illustrated in Figure 1.

The analysis of various baseline factors for potential contribution to overall survival is shown in Table 2. The factors associated with overall survival on univariate analysis were plasma levels of chromogranin-A (cutoff, 600 $\mu\text{g/L}$) and neuron-specific enolase

(NSE) (cutoff, 25 $\mu\text{g/L}$; Fig. 2), hepatic tumor burden, Ki-67 index (pG1–pG3), and ^{18}F -FDG uptake (mG1–mG3) at baseline. On multivariate analysis, only the baseline NSE plasma level ($P = 0.016$) and ^{18}F -FDG uptake ($P = 0.015$) remained as independent factors of overall survival. A plasma NSE level of at least 25 $\mu\text{g/L}$ at baseline was associated with a hazard ratio (HR) of 2.9 (95% CI, 1.2–7.0). For metabolic grading (mG1–mG3), the mG1 group had to be withheld from multivariate analysis because of missing events, but even when only mG2 and mG3 were considered, the metabolic stratification system remained significant for survival: mG3 status (T/L SUV ratio > 2.3) was an independent predictor, with an HR of 4.7 (95% CI, 1.2–7.0). An alternative cutoff for hepatic tumor burden, 50% of liver volume instead of 25%, again yielded nonsignificant results ($P > 0.3$) on multivariate analysis despite its univariate significance (log-rank, $P < 0.001$).

The well-established G1–G3 stratification system by Ki-67 immunostaining (1,3)—here termed pG1–G3 for pathologic grading—and the corresponding metabolic grading into mG1–mG3 (Table 3) both significantly correlated with overall survival in the suggested strata (Table 2; Figs. 3 and 4). The correlation of Ki-67–based and metabolic grading is shown in Figure 5. The presented data should not be confused with a lesion-based comparison of proliferation index and glucometabolic activity; the pathologic grading was performed punctually on a single, sometimes resected, lesion whereas metabolic grading was derived from the actual whole-body imaging, on which the glucose-avid target lesion was the relevant one for classification.

The additional analysis of the G1–G2 cohort with gastrointestinal NET in the strict (i.e., nonpulmonary) sense was performed after exclusion of patients with G3 NENs or with a pulmonary primary tumor. In this analysis, metabolic grading remained the only significant risk factor ($P = 0.042$); none of the other variables, including Ki-67 grading (G1 vs. G2), had a significant prognostic impact (hepatic tumor burden $> 25\%$, $P = 0.088$; plasma chromogranin-A $\geq 600 \mu\text{g/L}$, $P = 0.355$; Ki-67–based G2 grading, $P = 0.306$). The same analysis for SUV_{max} (instead of the T/L SUV ratio) yielded nonsignificant results on multivariate analysis, with P being 0.408 (SUV as a continuous variable) or 0.501 (categorical implementation as mG1–mG3 for SUV_{max} of <2.5 , 2.5–6.0, or >6.0).

DISCUSSION

This retrospective dual-center study on 89 stage IV gastroenteropancreatic NEN patients demonstrated the prognostic value of ^{18}F -FDG PET and—for the first time, to our knowledge—the feasibility of noninvasive metabolic grading into 3 risk categories using the proposed methodology. We were able to show that these molecular imaging–derived grades (mG1, mG2, and mG3) correlated inversely with survival and that stratification was the strongest independent separator for overall survival in the palliative setting. Although the only existing studies indicating ^{18}F -FDG PET to have prognostic value were both performed on mixed cohorts consisting of 38 (20) and 85 (19) patients with metastasized disease, our study investigated only gastroenteropancreatic NEN stage IV with inoperable metastatic disease, as this condition represents the largest therapeutic challenge and

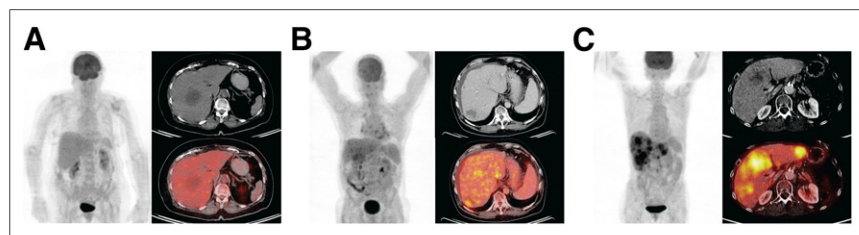


FIGURE 1. Examples of different metabolic grading classes with maximum-intensity-projection whole-body ^{18}F -FDG PET (left), transaxial CT (top), and transaxial PET/CT (bottom). (A) G2 gastroenteropancreatic NET of unknown origin (Ki-67 index, 10%; mG1) in patient who was alive after 29 mo (end of study, 29 mo+). (B) G1 NET with bronchial primary (Ki-67 index, 1%; mG2; T/L SUV ratio, 2.3) in patient who was alive at 26 mo (end of study, 26 mo+). (C) G2 NET with pancreatic primary (Ki-67 index, 20%; mG3; T/L SUV ratio, 4.0) in patient who died after 3 mo.

TABLE 2
Uni- and Multivariate Analyses of Potential Factors Contributing to Overall Survival

Factor	<i>n</i>	%	Overall survival (mo)		Univariate analysis (<i>P</i>)	Multivariate analysis		
			Median	95% CI		HR	95% CI	<i>P</i>
All patients	89	100.0	29	21–37				
Age								
≤65 y	51	57.3	31	19–43	0.193			
>65 y	38	42.6	25	5–45				
Tumor origin								
Pancreatic NEN	31	35.2	21	10–31	0.144			
Gastrointestinal NEN	57	64.8	31	13–49				
Foregut	46	52.3	30	9–51				
Midgut	16	18.2	NR		0.215			
Hindgut	4	4.5	8	0–41				
Unknown primary	22	25.0	14	6–22				
Pathologic grading (Ki-67 index)								
pG1 (≤2%)	16	20.0	NR					
pG2 (3%–20%)	46	57.5	28	0–62	<0.001	2.2	0.6–8.0	0.252
pG3 (>20%)	18	22.5	10	4–16		2.8	0.7–11.2	0.157
Karnofsky index								
>70	20	29.4	31	13–49	0.116			
≤70	48	70.6	13	10–16				
Tumor burden (liver)								
≤25%	63	74.1	40	7–73	0.002	1.3	0.4–4.0	0.669
>25%	22	25.9	11	0–28				
Metabolic grading (T/L SUV ratio)								
mG1 (≤1)	9	10.2	NR				*	*
mG2 (>1–2.3)	22	25.0	14	27–83	<0.001	4.7	1.3–16.1	0.015
mG3 (>2.3)	57	64.8	4	6–20				
Chromogranin A								
<600 µg/L	33	55.9	NR		0.011	1.5	0.7–3.6	0.336
≥600 µg/L	26	44.1	22	1–43				
NSE								
<25 µg/L	35	59.3	56	11–101	0.003	2.9	1.2–7.0	0.016
≥25 µg/L	24	40.7	10	6–14				

*Missing events in mG1 group.

NR = not reached.

probably benefits most from whole-body metabolic imaging with regard to individualized treatment.

¹⁸F-FDG PET—besides its use for accurate staging and monitoring of treatment response—allows biologic tumor characterization and investigation of malignant potential and tumor viability by molecular imaging of the tumor's glucose metabolism (22). The prognostic impact has been demonstrated for several tumor entities in different settings, including lung cancer, melanoma, colorectal cancer, head and neck cancer, and esophageal cancer (11,23,24). For NETs, the use of ¹⁸F-FDG PET or PET/CT has been restricted and replaced by somatostatin receptor-mediated functional imaging because of the frequent presence of ¹⁸F-FDG-negative lesions. However, there are promising initial data available (19,20) indicating a worse outcome in ¹⁸F-FDG-avid NENs. The attractive feature of this imaging tool is that it provides noninvasive whole-body information allowing identification of the most aggressive lesions, on which metabolic grading is then based. This concept of relying on metabolic target lesions (¹⁸F-FDG metabolic hot spots within the body) for prognostication resembles in a macroscopic way the principle of immunohistochemical grading (Ki-67 index estimation), in which only the proliferative

hot spots within a tumor are chosen to determine the proliferative fraction. Including the most aggressive and probably prognostically relevant lesions in tumor heterogeneity or diverging tumor populations may become of increasing importance in later stages of metastatic disease (10), and thus, whole-body molecular imaging-based surveillance might constitute an advantage over proliferation assessment based on non-PET-guided biopsy (25–27). The value of ¹⁸F-FDG PET in NENs seems of particular interest during the unresectable metastatic stage, as investigated in our study.

In this study cohort, the proposed metabolic grading system according to tumor ¹⁸F-FDG avidity proved highly prognostic and superior to other parameters, including hepatic tumor burden, plasma chromogranin-A and NSE level, and standard Ki-67-derived grading (pG1–pG3). On multivariate analysis (Table 2), PET-based metabolic grading (Table 3) remained the only independent prognostic factor (HR, 4.7; *P* = 0.015) besides a markedly elevated plasma NSE level (HR, 2.9; *P* = 0.016; Fig. 2). This finding indicates the strong predictive character for survival associated with the degree of ¹⁸F-FDG avidity in NENs regardless of the extent of metastatic disease and other known prognostic variables. Patients with markedly increased ¹⁸F-FDG uptake in the tumor

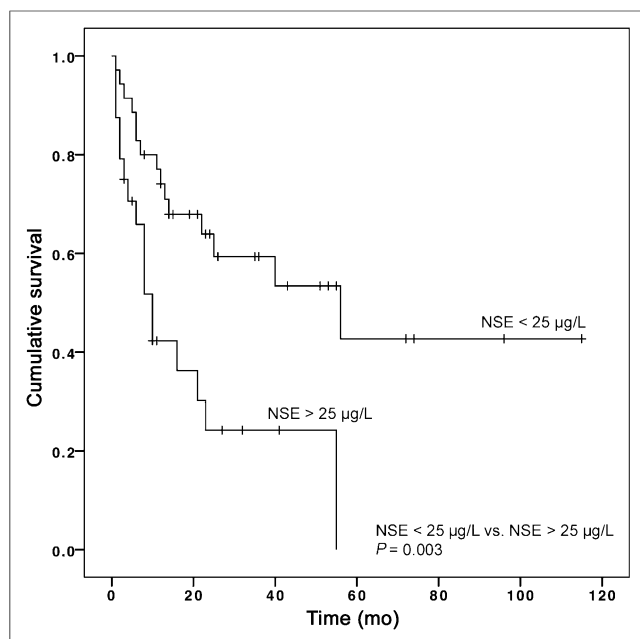


FIGURE 2. Overall survival of metastatic gastroenteropancreatic NEN patients stratified by baseline NSE plasma level (cutoff, 25 µg/L). Patients with markedly elevated plasma NSE had significantly shorter overall survival (median, 2 mo) than remaining patients (median, 23 mo).

as compared with the healthy liver (T/L SUV ratio > 2.3; that is, mG3) will have a significantly shorter overall survival than ^{18}F -FDG-negative patients, that is, individuals with no increased tumor uptake (mG1). This fact may have implications for selecting an adequate systemic treatment option, for example, aggressive (platinum-based) versus less aggressive regimens.

Looking at the prognostic impact of the investigated variables in the cohort of strict gastrointestinal NET patients (G1–G2), that is, after exclusion of NENs with a pulmonary primary tumor and of G3 NENs, the multivariate analysis reveals metabolic grading as the only independent factor with a significant impact on survival ($P = 0.042$). This analysis substantiates that the metabolic information based on maximum glucose avidity of tumors does in fact have an important prognostic impact even in well-differentiated gastrointestinal NETs of a G1–G2 grade; this finding is noteworthy because these low-grade tumors are believed to be suboptimal candidates for imaging with ^{18}F -FDG because of a reduced uptake propensity and thus poor sensitivity.

TABLE 3

Definition of Pathologic and Metabolic Grading in This Study

Pathologic		Metabolic	
Grade	Ki-67 index	Grade	T/L SUV ratio*
pG1	≤2%	mG1	<1
pG2	3–20%	mG2	1–2.3
pG3	>20%	mG3	>2.3

*T/L ratio of SUV_{max} .

Pathologic grading is according to TNM staging and grading system for NET; metabolic grading is proposal according to ^{18}F -FDG PET/CT (own data).

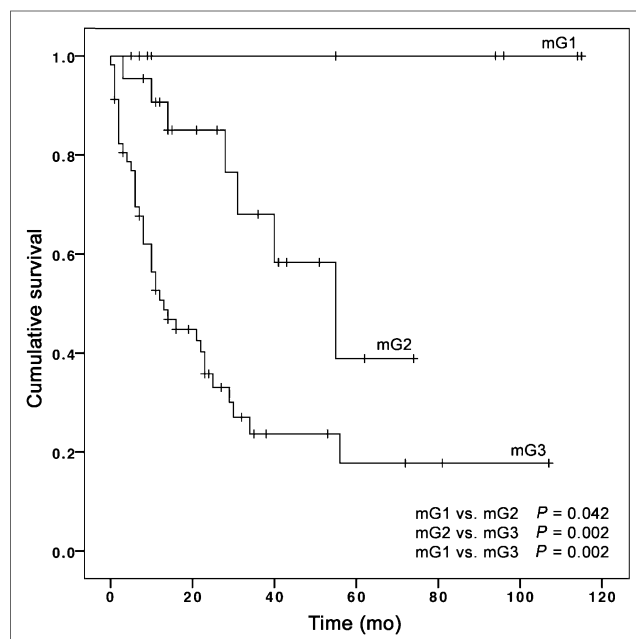


FIGURE 3. Impact of metabolic grading on overall survival as illustrated by Kaplan-Meier curves after stratification by T/L SUV ratio. Patients with T/L SUV ratio of 1–2.3 (mG2) and >2.3 (mG3) had median overall survival of 55 mo (95% CI, 27.2–82.9) and 13 mo (95% CI, 6.1–19.9), respectively. Median overall survival for patients with T/L SUV ratio < 1 (mG1) was not reached after 114 mo. Log-rank test was significant for all comparisons.

The limited correlation of the patients' Ki-67 index and the metabolic grading derived from whole-body molecular imaging (Fig. 5) further illustrates the main point of this study, shown by the above-mentioned multivariate analysis: the independent prognostic value of ^{18}F -FDG PET in advanced (stage IV) gastrointestinal NENs, in particular independent of the immunohistochemical (Ki-67-based) grading. However, this investigation clearly cannot provide any proof of prognostic superiority of PET over the standard grading method; the retrospectively chosen cutoffs for metabolic grading (mG1–mG3), as well as the interval between immunohistochemical assessment (pG grading) and molecular imaging (mG grading), are prohibitive of any conclusions in this direction. The mentioned time gap (mean, 8.4 mo) will probably not have markedly distorted the results but certainly presents a bias in favor of molecular imaging.

There are 2 reports proposing the baseline plasma NSE level as a potential risk factor for survival in patients with metastatic NENs (9,28). There is no well-established explanation for this phenomenon, but an inverse relation between tumor differentiation and plasma NSE levels in NENs was reported earlier (29) and substantiated in a recent larger study (30). Because our data confirm the negative prognostic impact of markedly elevated plasma NSE levels (>25 µg/L), which were the only other independent predictor of survival in our cohort of inoperable patients (HR, 2.9; $P = 0.016$), studies should be designed to further investigate the potential role of this baseline biomarker for patient management. Another generally important predictor, hepatic tumor burden, did not persist as a major prognostic factor on multivariate analysis. The selected and common cutoff of 25% liver volume replacement, however, seemed not to be the reason for its insignificant prognostic penetrance. The 50% cutoff performed similarly suboptimally despite

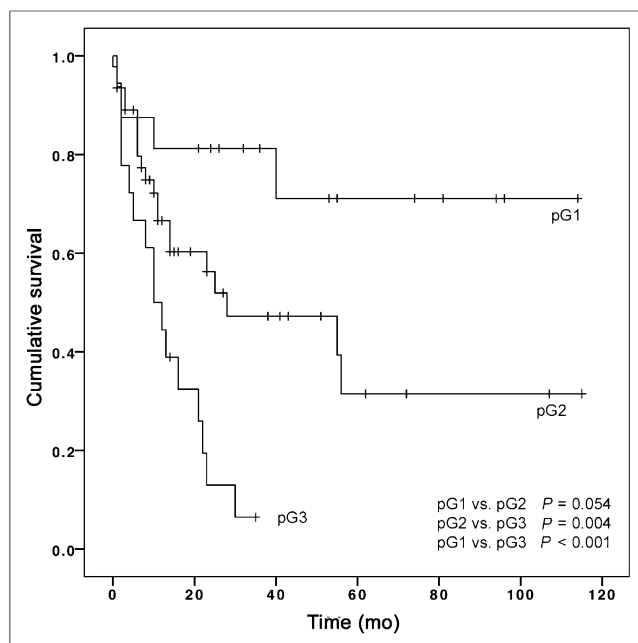


FIGURE 4. Impact of Ki-67–based histopathologic grading on overall survival as illustrated by Kaplan–Meier curves. Patients with Ki-67 index > 20% (G3), Ki-67 index of 3%–20% (G2), and Ki-67 index < 3% (G1) had median overall survival of 10 mo (95% CI, 4.5–15.5), 28 mo (95% CI, 0–61.9), and >114 mo, respectively. For G1 patients, median overall survival had not been reached after 114 mo.

univariate significance, potentially because of the small subgroup of patients with liver burden greater than 50% ($n = 9$).

The large percentage of patients with ^{18}F -FDG–positive NENs is probably due to the relatively high proportion of high-risk NENs in this study; the selection bias created by requiring ^{18}F -FDG PET/CT as an inclusion criterion is mentioned in the next paragraph. The significant proportion of high-risk NENs in our cohort is also reflected by the uncommon fraction of G3 NENs in our cohort.

Our study had several limitations. First, the ability to deduce conclusions from a retrospective analysis is generally limited. Particularly, the retrospective calculation of threshold values for ^{18}F -FDG is a main limitation. However, because of the lack of prospective study data in the field of NENs, most insights for prognostication—including the value of the Ki-67 index—have been derived from retrospective studies. Another limitation is

the inherent inaccuracy of the Ki-67 index regarding its timing and location. Although this reflects the clinicians' reality in the routine setting and in clinical studies that have demonstrated its prognostic value, ideally the parameter should be reassessed during the course of the disease. Such practice is often not routine, probably because of the invasiveness of the procedure. Third, the method of ^{18}F -FDG uptake quantification is subject to many sources of inaccuracy and inter- and intraindividual variation. Also, because CT was used to exclude sites of involvement when background regions of interest were placed, undetected tumor within the liver may have been included in the healthy liver background. Our study did not use partial-volume correction in PET image reconstruction, and the use of such an algorithm would definitely make SUV estimations more accurate and robust against lesion size reduction. Many technical improvements in PET should help improve the concept of metabolic grading in future studies, such as 4-dimensional acquisitions with respiration-gated algorithms and dual-time-point or even dynamic PET acquisitions to more accurately quantify and characterize the glucolytic metabolism of tumor lesions. The interval between ^{18}F -FDG injection and imaging may influence tumor uptake and the SUV ratio, thus resulting in skewed metabolic grading. There were no systematic differences in this parameter between the 2 institutions and no statistical divergence ($P > 0.2$). Use of the T/L SUV ratio instead of mere SUV_{max} may have an advantage in comparisons of different institutions but also introduces error via variations in uptake by healthy liver tissue; however, the robustness of the ratio parameter proved adequate for prognostic stratification in our study and performed better than SUV_{max} on multivariate analysis. We are aware of the selection bias caused by our inclusion criterion of an ^{18}F -FDG PET study; the tendency to perform this modality in cases with a suspected potential for risk will influence the cohort composition. However, the multivariate analysis after inclusion of other known risk factors substantiated the prognostic value of the method irrespective of the bias. It remains unclear when and how treatment was influenced by the results of PET imaging. This is another source of bias for the analysis. However, we think that the decline in outcome with increasing metabolic grade would not have been caused only by the difference in treatment.

CONCLUSION

This study demonstrated the strong independent prognostic value of ^{18}F -FDG PET in metastatic NENs. As shown by our

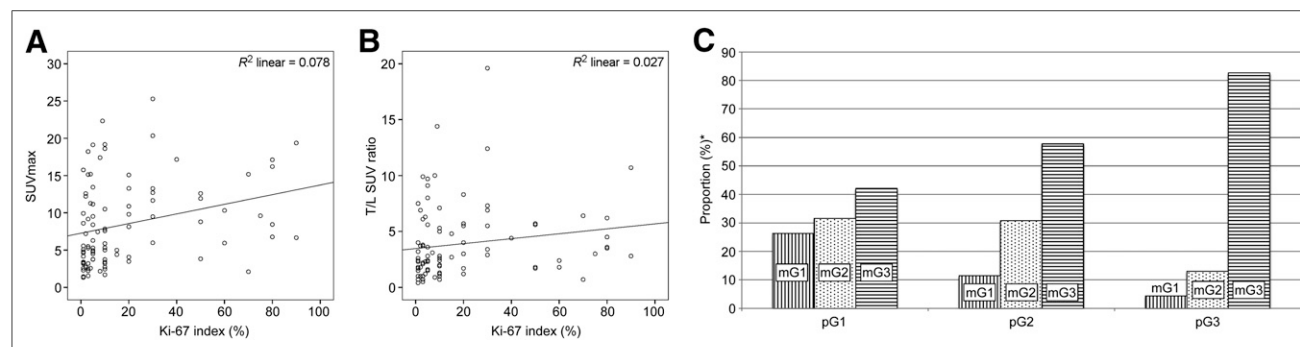


FIGURE 5. Association of proliferation index and whole-body imaging–derived target metabolic activity. (A) Correlation of patients' Ki-67 index and whole-body imaging–derived target SUV_{max} ($P = 0.007$, $r = 0.279$). (B) Same analysis with T/L SUV ratio instead of SUV ($P = 0.117$, $r = 0.163$). (C) Association of pathologic and metabolic grading. *Proportions of metabolic grading classes (mG grades) within each classic Ki-67–based grading category ($P = 0.004$, $r = 0.294$).

analysis, this modality allows metabolic grading into 3 different risk categories (mG1–mG3) with high predictive power regarding overall survival. We propose consideration of whole-body molecular imaging with ^{18}F -FDG PET as a noninvasive, effective grading method and as a complement to conventional Ki-67–based grading; the presumed value for guiding biopsy-based proliferation assessments in metastatic disease should be further investigated. Future studies should eventually define the role of metabolic grading for individualizing treatment and for tailoring the aggressiveness of systemic therapy, for example, platinum-based (cytoreductive) chemotherapies versus less aggressive (antiproliferative) systemic treatments such as everolimus.

DISCLOSURE

The costs of publication of this article were defrayed in part by the payment of page charges. Therefore, and solely to indicate this fact, this article is hereby marked “advertisement” in accordance with 18 USC section 1734. No potential conflict of interest relevant to this article was reported.

REFERENCES

- Rindi G, Kloppel G, Couvelard A, et al. TNM staging of midgut and hindgut (neuro) endocrine tumors: a consensus proposal including a grading system. *Virchows Arch*. 2007;451:757–762.
- Rindi G, Kloppel G, Alhman H, et al. TNM staging of foregut (neuro)endocrine tumors: a consensus proposal including a grading system. *Virchows Arch*. 2006;449:395–401.
- Klöppel G, Couvelard A, Perren A, et al. ENETS consensus guidelines for the standards of care in neuroendocrine tumors: towards a standardized approach to the diagnosis of gastroenteropancreatic neuroendocrine tumors and their prognostic stratification. *Neuroendocrinology*. 2009;90:162–166.
- Pape UF, Perren A, Niederle B, et al. ENETS consensus guidelines for the management of patients with neuroendocrine neoplasms from the jejunum-ileum and the appendix including goblet cell carcinomas. *Neuroendocrinology*. 2012;95:135–156.
- Pavel M, Baudin E, Couvelard A, et al. ENETS consensus guidelines for the management of patients with liver and other distant metastases from neuroendocrine neoplasms of foregut, midgut, hindgut, and unknown primary. *Neuroendocrinology*. 2012;95:157–176.
- Falconi M, Bartsch DK, Eriksson B, et al. ENETS consensus guidelines for the management of patients with digestive neuroendocrine neoplasms of the digestive system: well-differentiated pancreatic non-functioning tumors. *Neuroendocrinology*. 2012;95:120–134.
- Ezziddin S, Opitz M, Attassi M, et al. Impact of the Ki-67 proliferation index on response to peptide receptor radionuclide therapy. *Eur J Nucl Med Mol Imaging*. 2011;38:459–466.
- Ezziddin S, Sabet A, Heinemann F, et al. Response and long-term control of bone metastases after peptide receptor radionuclide therapy with ^{177}Lu -octreotate. *J Nucl Med*. 2011;52:1197–1203.
- Ezziddin S, Attassi M, Yong-Hing CJ, et al. Predictors of long-term outcome in patients with well-differentiated gastroenteropancreatic neuroendocrine tumors after peptide receptor radionuclide therapy with ^{177}Lu -octreotate. *J Nucl Med*. 2014;55:183–190.
- Basu S, Kwee TC, Gatenby R, Saboury B, Torigian DA, Alavi A. Evolving role of molecular imaging with PET in detecting and characterizing heterogeneity of cancer tissue at the primary and metastatic sites, a plausible explanation for failed attempts to cure malignant disorders. *Eur J Nucl Med Mol Imaging*. 2011;38:987–991.
- Smyth EC, Shah MA. Role of ^{18}F 2-fluoro-2-deoxyglucose positron emission tomography in upper gastrointestinal malignancies. *World J Gastroenterol*. 2011;17:5059–5074.
- Weber WA. Positron emission tomography as an imaging biomarker. *J Clin Oncol*. 2006;24:3282–3292.
- Kim BK, Kang WJ, Kim JK, et al. ^{18}F -fluorodeoxyglucose uptake on positron emission tomography as a prognostic predictor in locally advanced hepatocellular carcinoma. *Cancer*. 2011;117:4779–4787.
- Higashi T, Hatano E, Ikai I, et al. FDG PET as a prognostic predictor in the early post-therapeutic evaluation for unresectable hepatocellular carcinoma. *Eur J Nucl Med Mol Imaging*. 2010;37:468–482.
- Oyama N, Akino H, Suzuki Y, et al. Prognostic value of 2-deoxy-2-[^{18}F]fluoro-D-glucose positron emission tomography imaging for patients with prostate cancer. *Mol Imaging Biol*. 2002;4:99–104.
- Meirelles GS, Schoder H, Ravizzini GC, et al. Prognostic value of baseline [^{18}F] fluorodeoxyglucose positron emission tomography and $^{99\text{m}}\text{Tc}$ -MDP bone scan in progressing metastatic prostate cancer. *Clin Cancer Res*. 2010;16:6093–6099.
- Otomi Y, Otsuka H, Morita N, et al. Relationship between FDG uptake and the pathological risk category in gastrointestinal stromal tumors. *J Med Invest*. 2010;57:270–274.
- Park JW, Cho CH, Jeong DS, Chae HD. Role of F-fluoro-2-deoxyglucose positron emission tomography in gastric GIST: predicting malignant potential preoperatively. *J Gastric Cancer*. 2011;11:173–179.
- Binderup T, Knigge U, Loft A, Federspiel B, Kjaer A. ^{18}F -fluorodeoxyglucose positron emission tomography predicts survival of patients with neuroendocrine tumors. *Clin Cancer Res*. 2010;16:978–985.
- Garin E, Le Jeune F, Devillers A, et al. Predictive value of ^{18}F -FDG PET and somatostatin receptor scintigraphy in patients with metastatic endocrine tumors. *J Nucl Med*. 2009;50:858–864.
- Rindi G. The ENETS guidelines: the new TNM classification system. *Tumori*. 2010;96:806–809.
- Jaini S, Dadachova E. FDG for therapy of metabolically active tumors. *Semin Nucl Med*. 2012;42:185–189.
- Poeppl TD, Krause BJ, Heusner TA, Boy C, Bockisch A, Antoch G. PET/CT for the staging and follow-up of patients with malignancies. *Eur J Radiol*. 2009;70:382–392.
- Kwee TC, Basu S, Saboury B, Ambrosini V, Torigian DA, Alavi A. A new dimension of FDG-PET interpretation: assessment of tumor biology. *Eur J Nucl Med Mol Imaging*. 2011;38:1158–1170.
- Klaeser B, Mueller MD, Schmid RA, Guevara C, Krause T, Wiskirchen J. PET-CT-guided interventions in the management of FDG-positive lesions in patients suffering from solid malignancies: initial experiences. *Eur Radiol*. 2009;19:1780–1785.
- Klaeser B, Wiskirchen J, Wartenberg J, et al. PET/CT-guided biopsies of metabolically active bone lesions: applications and clinical impact. *Eur J Nucl Med Mol Imaging*. 2010;37:2027–2036.
- Werner MK, Aschoff P, Reimold M, Pfannenberger C. FDG-PET/CT-guided biopsy of bone metastases sets a new course in patient management after extensive imaging and multiple futile biopsies. *Br J Radiol*. 2011;84:e65–e67.
- Yao JC, Pavel M, Phan AT, et al. Chromogranin A and neuron-specific enolase as prognostic markers in patients with advanced pNET treated with everolimus. *J Clin Endocrinol Metab*. 2011;96:3741–3749.
- Baudin E, Gigliotti A, Ducreux M, et al. Neuron-specific enolase and chromogranin A as markers of neuroendocrine tumours. *Br J Cancer*. 1998;78:1102–1107.
- Korse CM, Taal BG, Vincent A, et al. Choice of tumour markers in patients with neuroendocrine tumours is dependent on the histological grade: a marker study of chromogranin A, neuron specific enolase, progastrin-releasing peptide and cytokeratin fragments. *Eur J Cancer*. 2012;48:662–671.



The Journal of
NUCLEAR MEDICINE

Prognostic Stratification of Metastatic Gastroenteropancreatic Neuroendocrine Neoplasms by ^{18}F -FDG PET: Feasibility of a Metabolic Grading System

Samer Ezziddin, Linda Adler, Amir Sabet, Thorsten Dirk Pöppel, Florian Grabellus, Ali Yüce, Hans-Peter Fischer, Birgit Simon, Tobias Höller, Hans-Jürgen Biersack and James Nagarajah

J Nucl Med. 2014;55:1260-1266.

Published online: May 29, 2014.

Doi: 10.2967/jnumed.114.137166

This article and updated information are available at:

<http://jnm.snmjournals.org/content/55/8/1260>

Information about reproducing figures, tables, or other portions of this article can be found online at:

<http://jnm.snmjournals.org/site/misc/permission.xhtml>

Information about subscriptions to JNM can be found at:

<http://jnm.snmjournals.org/site/subscriptions/online.xhtml>

The Journal of Nuclear Medicine is published monthly.
SNMMI | Society of Nuclear Medicine and Molecular Imaging
1850 Samuel Morse Drive, Reston, VA 20190.
(Print ISSN: 0161-5505, Online ISSN: 2159-662X)

© Copyright 2014 SNMMI; all rights reserved.

 SOCIETY OF
NUCLEAR MEDICINE
AND MOLECULAR IMAGING